Supporting Information for

Water-Soluble Argentivorous Molecule

Yoichi Habata*, Yoko Okeda, Mari Ikeda, and Shunsuke Kuwahara

Department of Chemistry, Faculty of Science & Research Center for Materials with Integrated Properties, Toho University
2-2-1 Miyama, Funabashi, Chiba 274-8510, Japan

Table of Contents

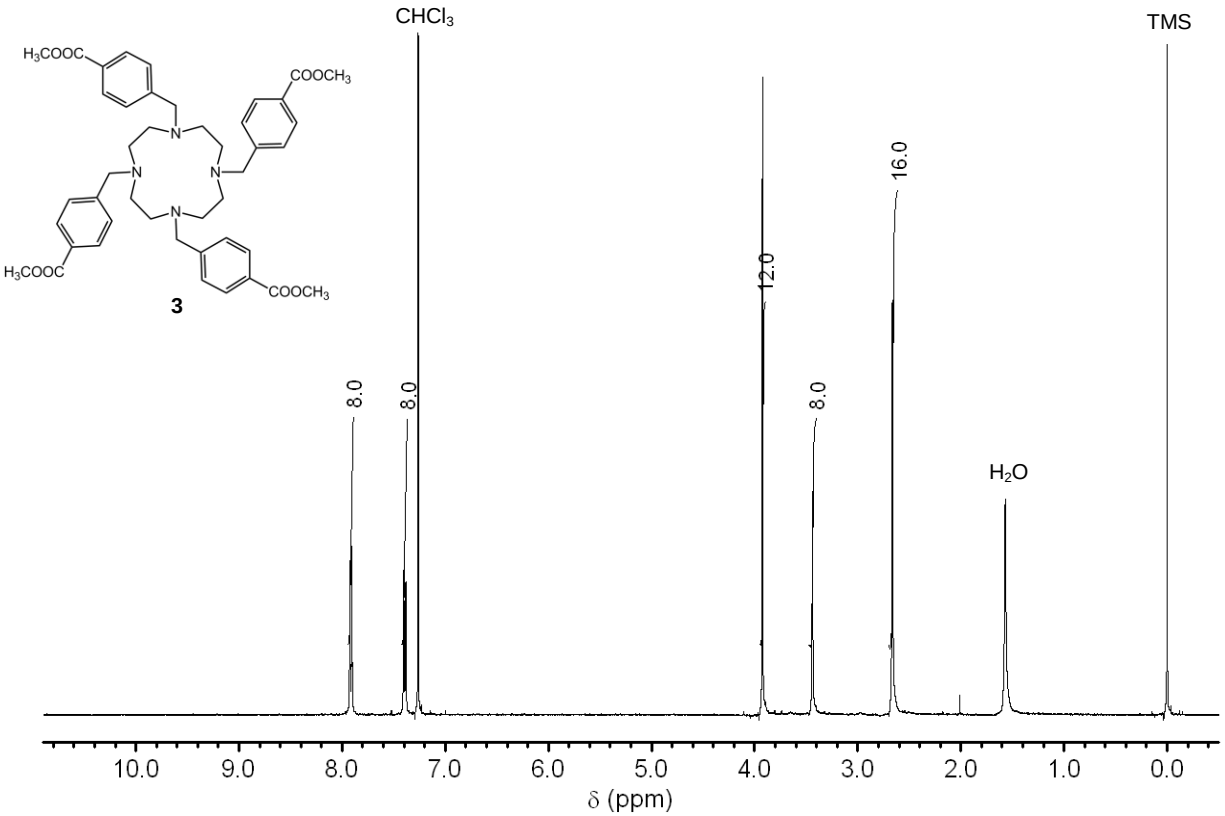

Figure S1. ^{1}H NMR of tetramethy 4,4',4",4"'-[1,4,7,10-tetraazacyclododecane-1,4,7,10-tetrayltetrakis (methylene)]tetrabenzoate (**3**) in $CDCl_3$ (298 K).

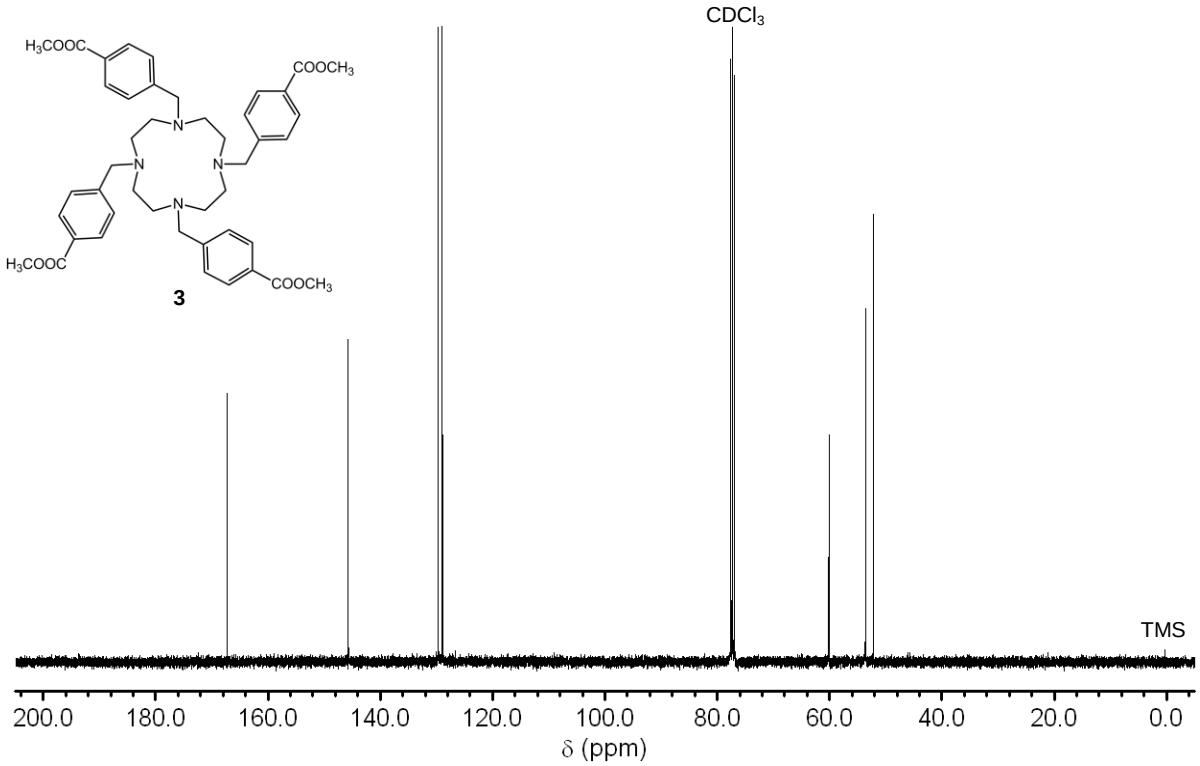

Figure S2. ^{13}C NMR of tetramethy 4,4',4",4"'-[1,4,7,10-tetraazacyclododecane-1,4,7,10-tetrayltetrakis (methylene)]tetrabenzoate (**3**) in $CDCl_3$ (298 K).

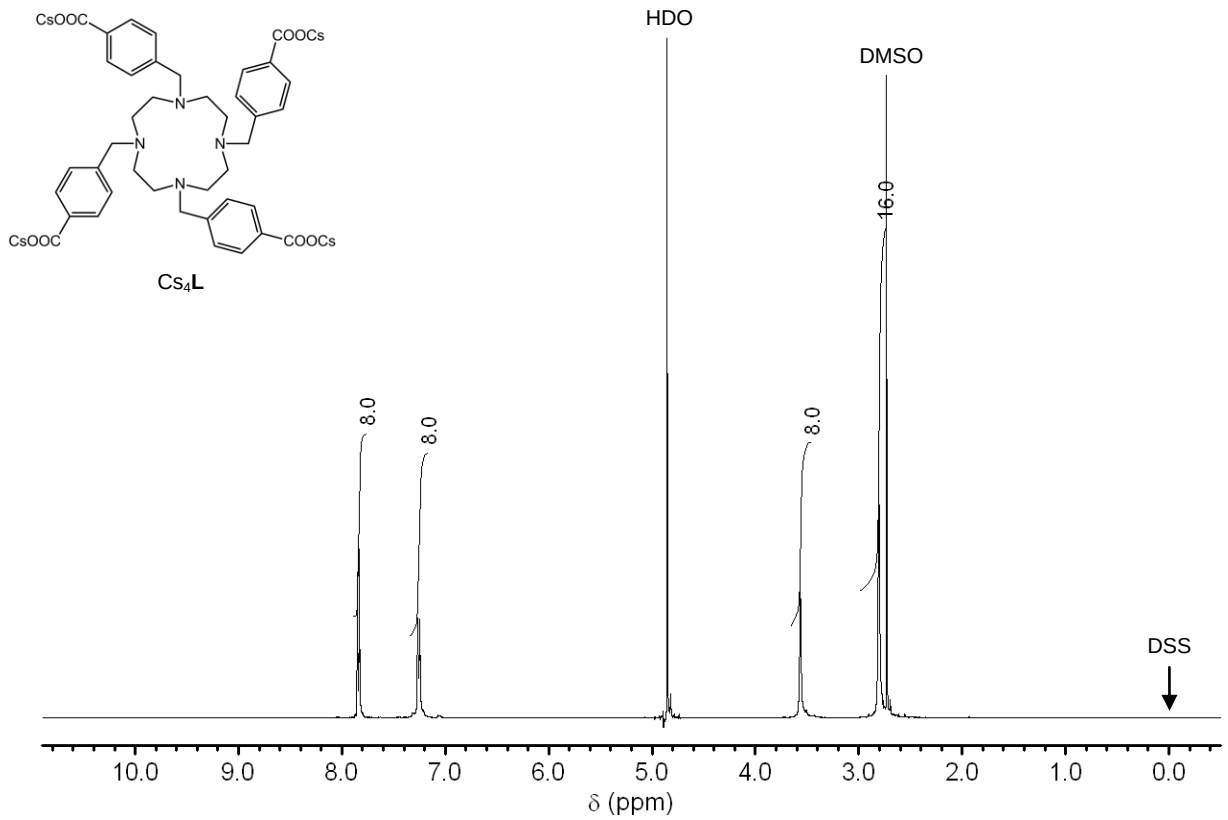

Figure S3. ^{1}H NMR of tetracesium 4,4',4",4"'-((1,4,7,10-tetraazacyclododecane-1,4,7,10-tetrayl) tetrakis (methylene))tetrabe-nzoate (Cs_4**L**) in D_2O. DSS(standard): Sodium 2,2-dimethyl-2-silapentane-5-sulfonate (298 K).

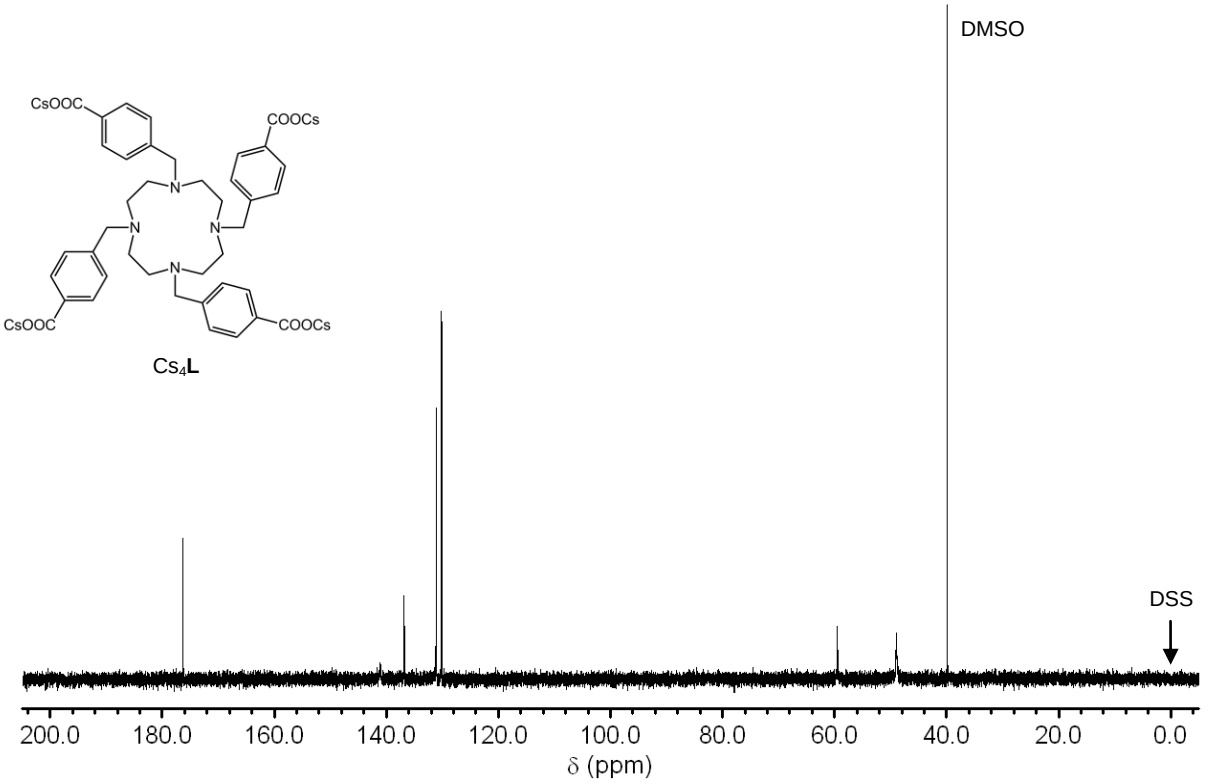

Figure S4. ^{13}C NMR of tetracesium 4,4',4",4"'-((1,4,7,10-tetraazacyclododecane-1,4,7,10-tetrayl) tetrakis (methylene))tetrabe-nzoate (Cs_4**L**) in D_2O. DSS(standard): Sodium 2,2-dimethyl-2-silapentane-5-sulfonate (298

K).

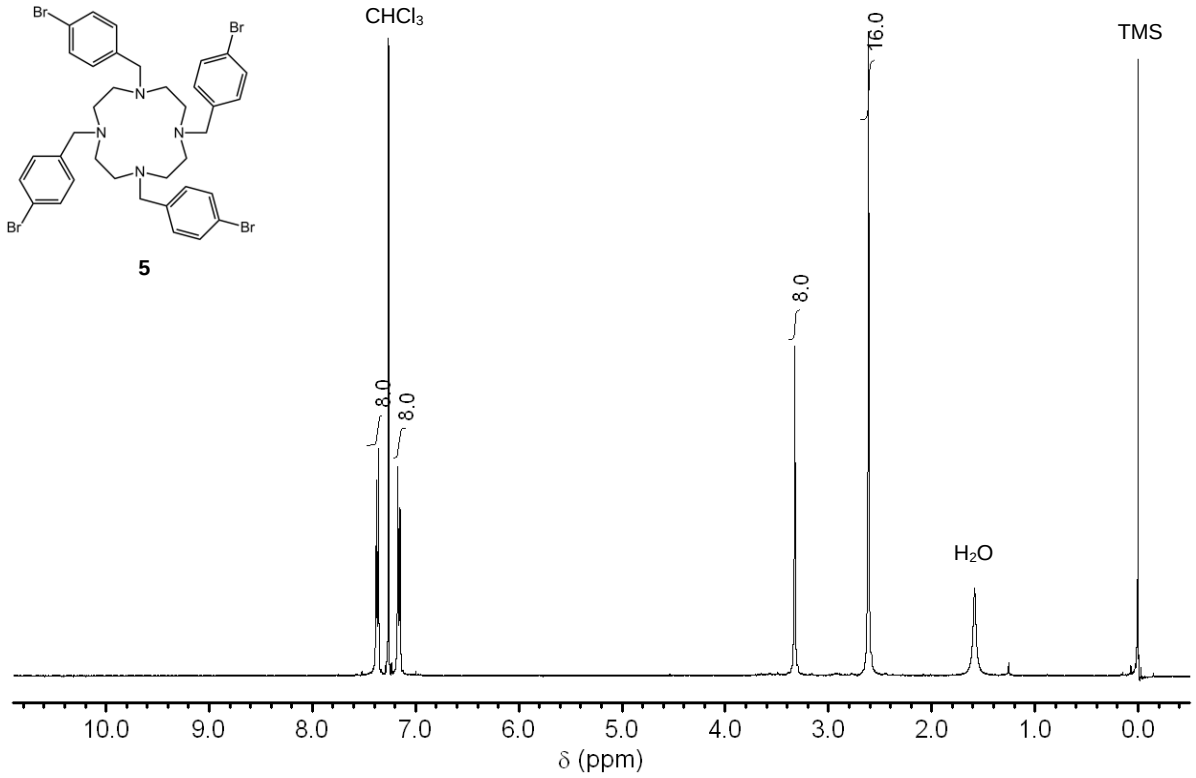

Figure S5. ^{1}H NMR of 1,4,7,10-tetrakis(4-bromobenzyl)-1,4,7,10-tetraazacyclododecane (**5**) in $CDCl_3$ (298 K).

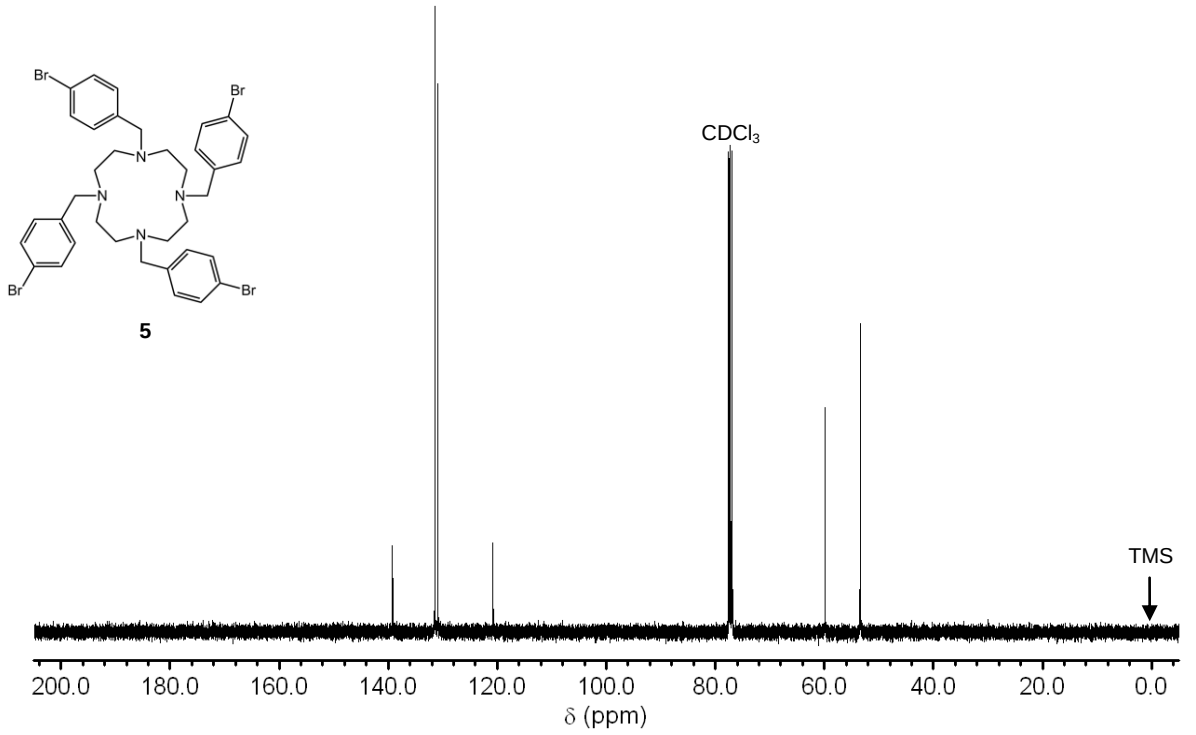

Figure S6. ^{13}C NMR of 1,4,7,10-tetrakis(4-bromobenzyl)-1,4,7,10-tetraazacyclododecane (**5**) in $CDCl_3$ (298 K).

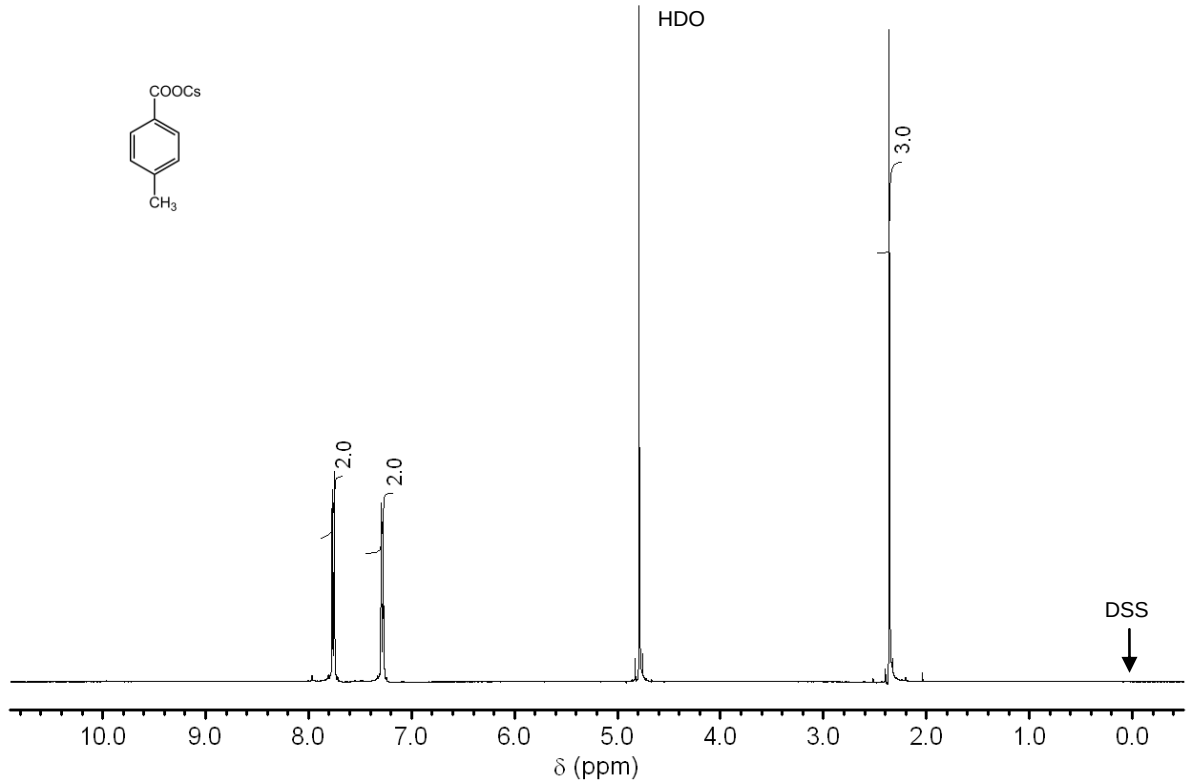

Figure S7. ^{1}H NMR of cesium 4-methylbenzoate in D_2O. DSS(standard): Sodium 2,2-dimethyl-2-silapentane-5-sulfonate (298 K).

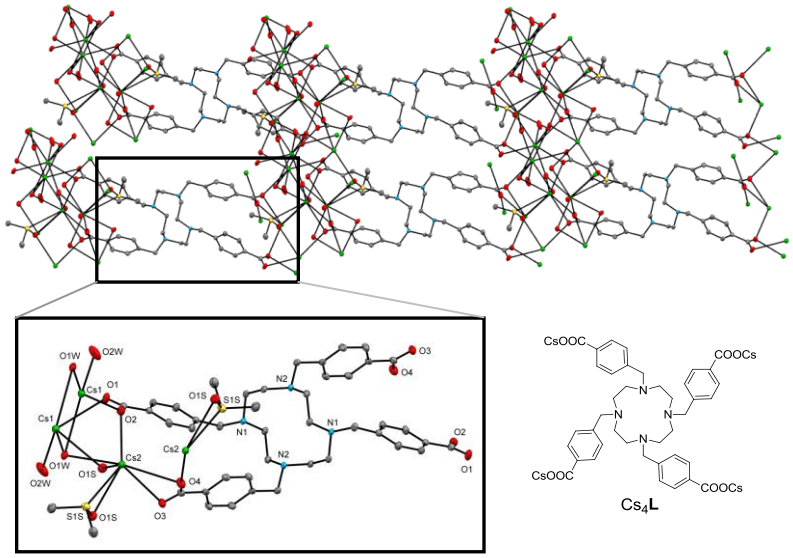

Figure S8. ORTEP diagrams of Cs_4**L**. (top) Packing diagram and (bottom) expanded diagram. Two waters and two DMSOs bind the cesium ions in Cs_4**L**. Hydrogen atoms omitted.

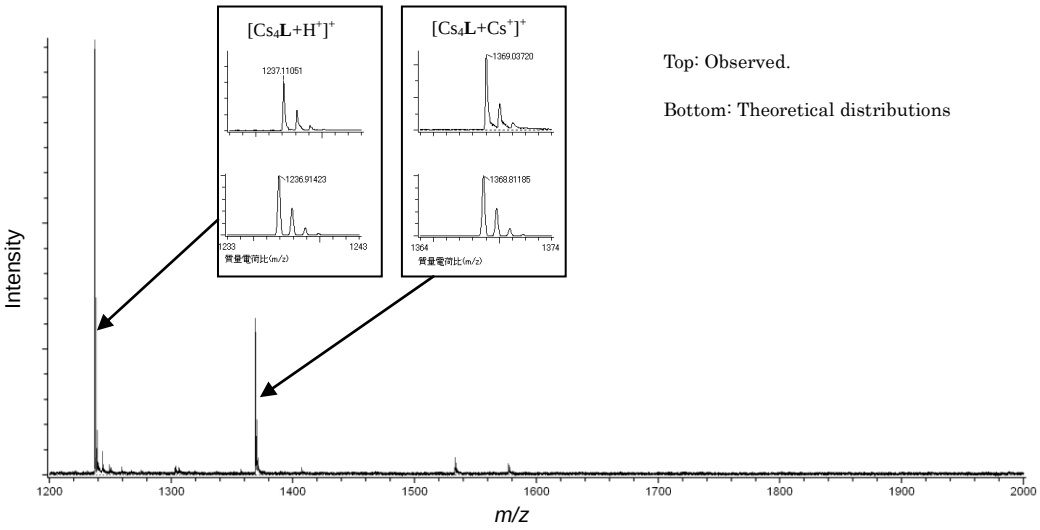

Figure S9. Cold ESI-MS of Cs_4**L** (H_2O:CH_3OH = 1:7).

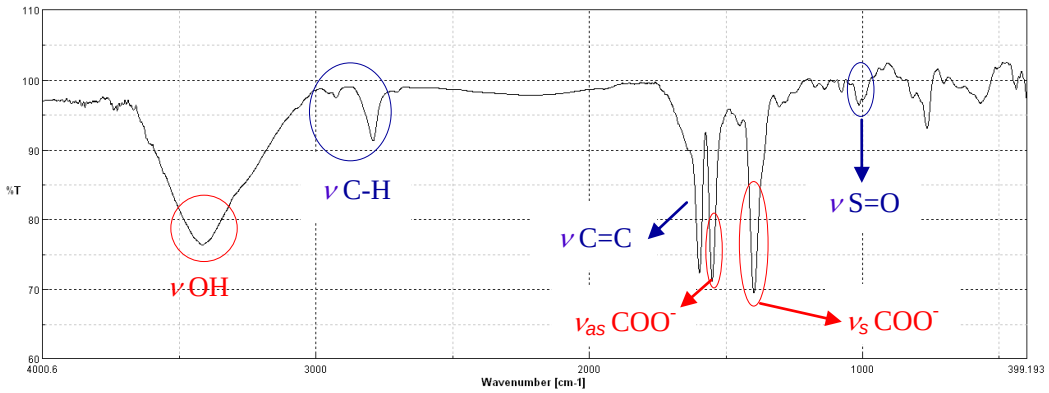

Figure S10. IR spectrum of Cs_4**L** (KBr disk). The IR data suggests that Cs_4**L** includes H_2O and DMSO.

Table S1. Crystal data and structure refinement for Cs_4**L**.

Identification code	Cs_4**L**	
Empirical formula	C22 H30 Cs2 N2 O7 S	
Formula weight	732.36	
Temperature	100 K	
Wavelength	0.71073 Å	
Crystal system	Triclinic	
Space group	P-1	
Unit cell dimensions	a = 8.9076(5) Å	α= 97.8800(10)°.
	b = 9.0591(5) Å	β= 103.7500(10)°.
	c = 17.7228(10) Å	γ = 102.0670(10)°.
Volume	1331.93(13) $Å^3$	
Z	2	
Density (calculated)	1.826 Mg/m^3	
Absorption coefficient	2.858 mm^{-1}	
F(000)	716	
Crystal size	0.26 x 0.17 x 0.03 mm3	
Theta range for data collection	1.21 to 27.48°.	
Index ranges	-11<=h<=11, -8<=k<=11, -22<=l<=20	
Reflections collected	8549	
Independent reflections	6039 [R(int) = 0.0161]	
Completeness to theta = 27.48 ⁻	98.7 %	
Absorption correction	Empirical	
Max. and min. transmission	0.9091 and 0.5203	
Refinement method	Full-matrix least-squares on F^2	
Data / restraints / parameters	6039 / 0 / 325	
Goodness-of-fit on F2	1.134	
Final R indices [I>2sigma(I)]	R1 = 0.0233, wR2 = 0.0621	
R indices (all data)	R1 = 0.0287, wR2 = 0.0723	
Largest diff. peak and hole	0.672 and -0.840 e. $Å^{-3}$	

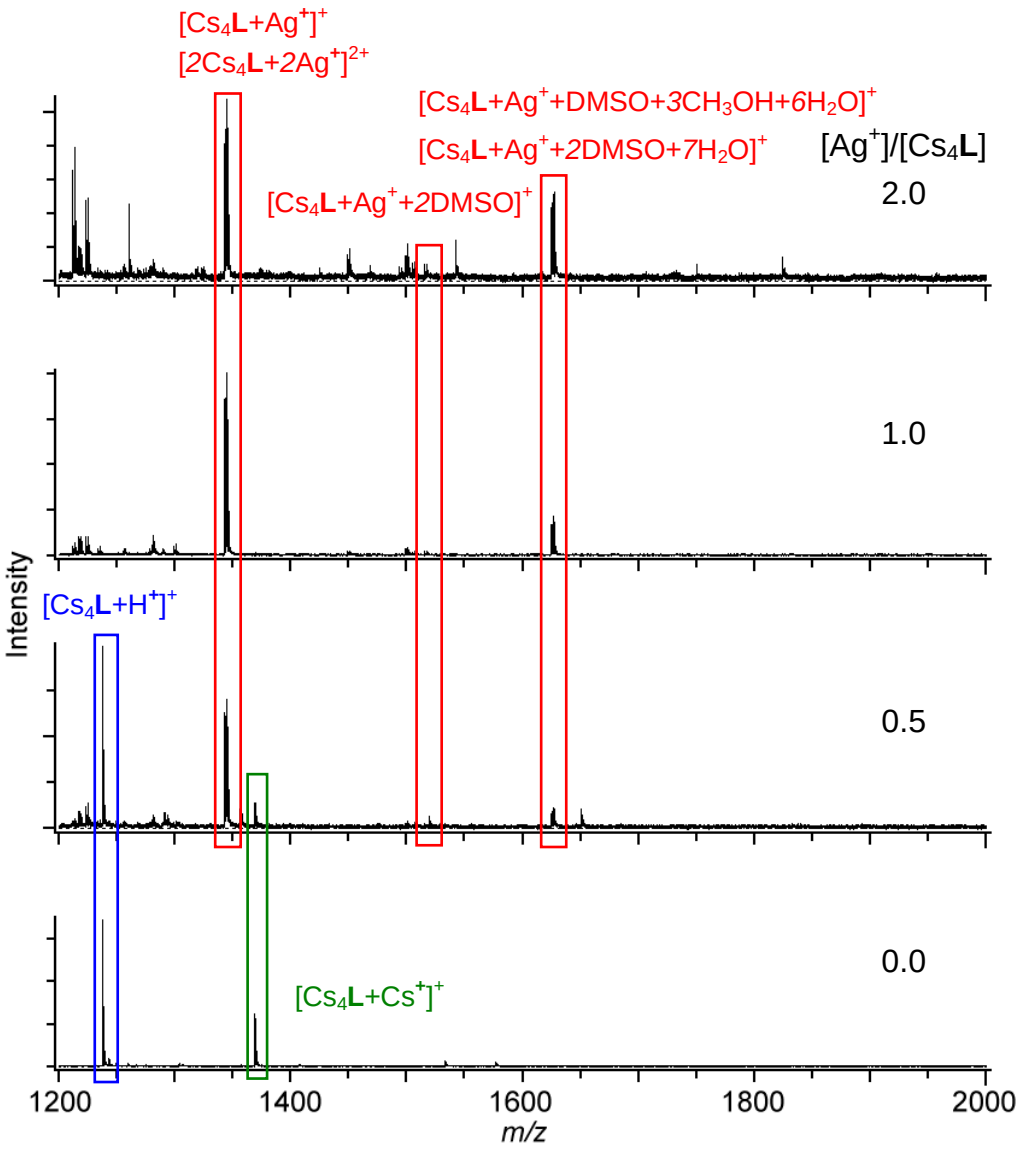

Figure S11a. Ag^+-ion-induced Cold ESI-Mass spectral changes (CH_3OH, 298 K).

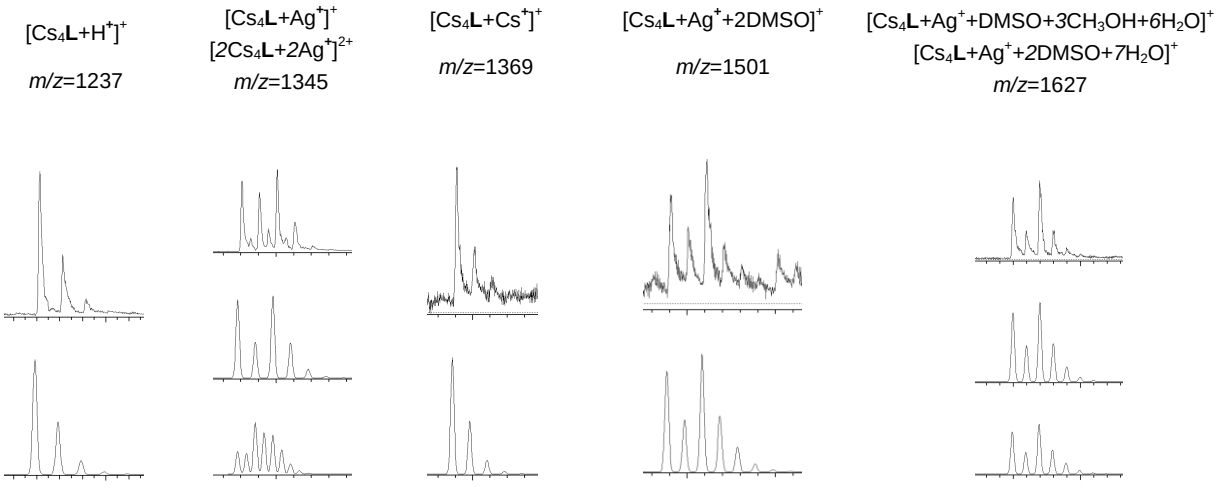

Figure S11b. Observed ion peaks (top) and theoretical distributions (bottom) in Figure S10a.

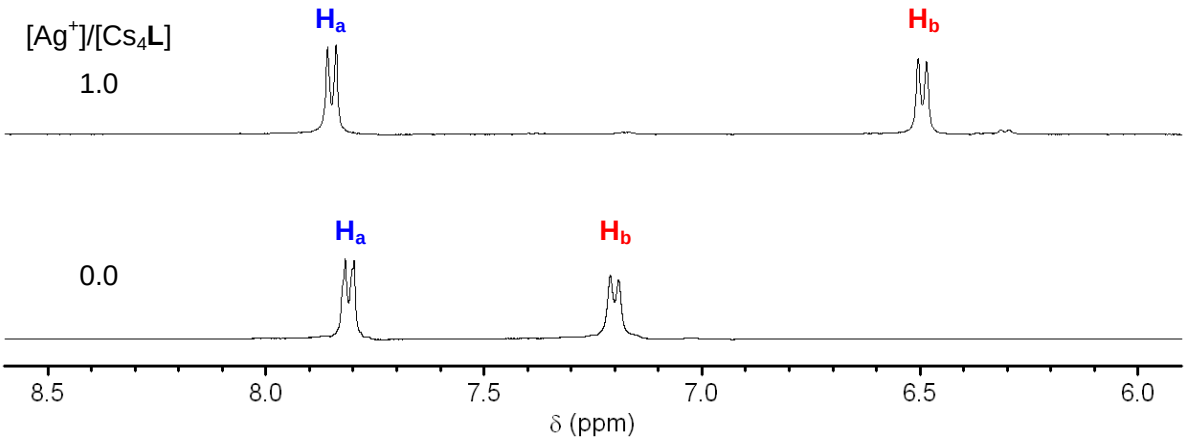

Figure S12. $AgCF_3SO_3$-induced ^{1}H-NMR spectral changes (D_2O, 298 K)

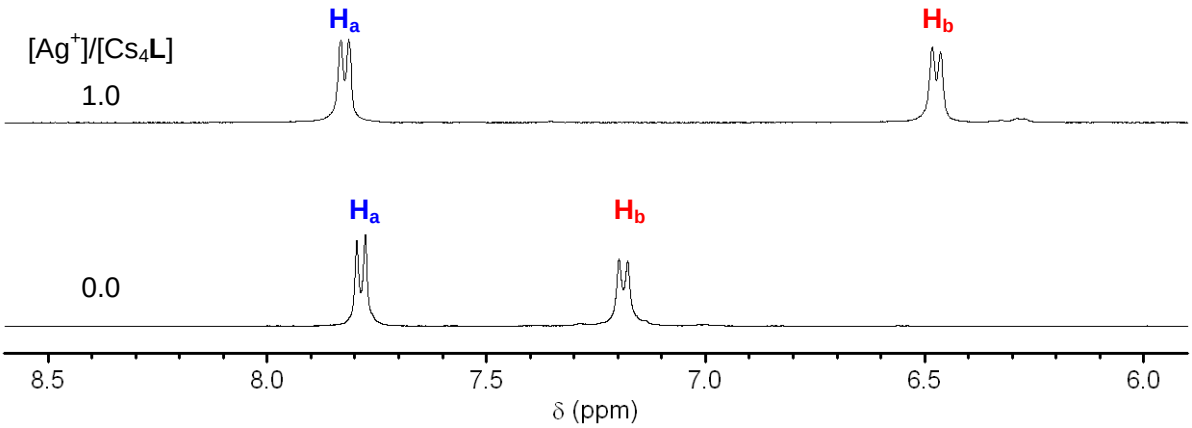

Figure S13. $AgPF_6$-induced ^{1}H-NMR spectral changes (D_2O, 298 K)

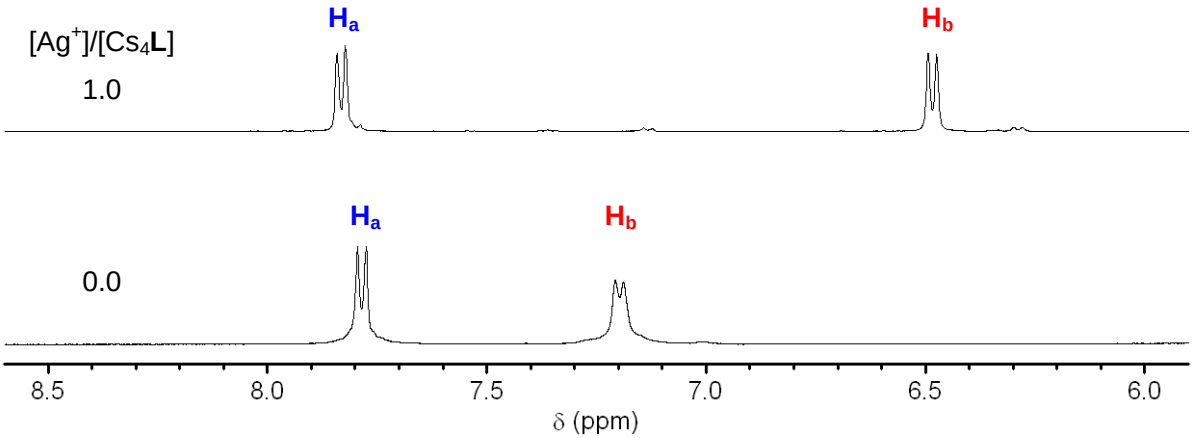

Figure S14. $AgNO_3$-induced ^{1}H-NMR spectral changes (D_2O, 298 K)

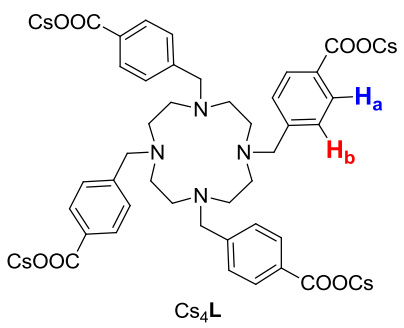

Table S2. ^{1}H NMR chemical shift changes of the protons at 2'-/6'- positions(H_b) (δ/ppm).

$AgCF_3SO_3$	-0.69
$AgPF_6$	-0.72
$AgNO_3$	-0.72

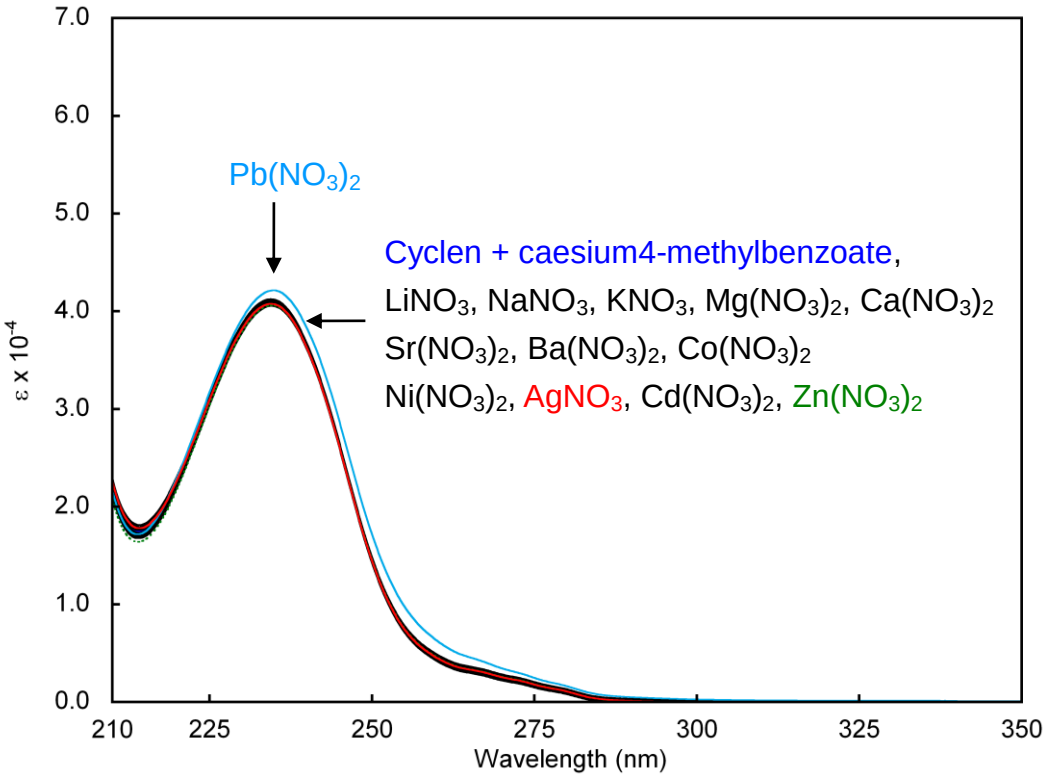

Figure S15. Pb^{2+}-induced UV spectral changes. (Cyclen : Cesium 4-methylbenzoate=1:4) [Cesium 4-methylbenzoate] = 2.0 x 10^{-4} mol/L (in water).

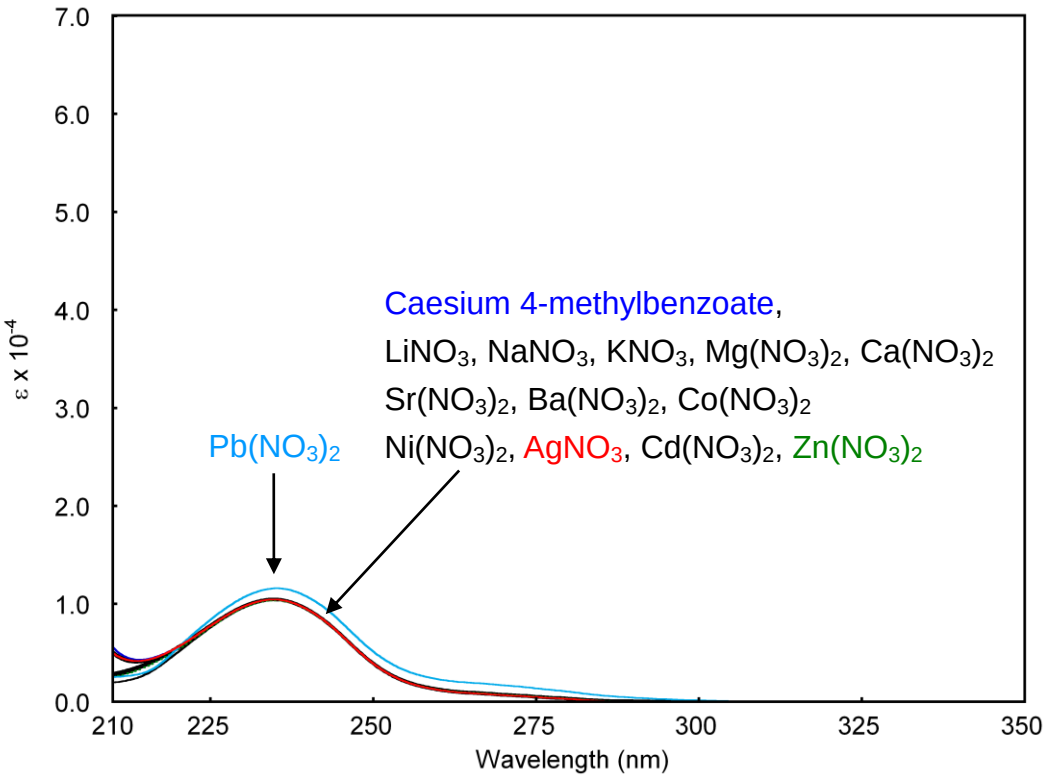

Figure S16. Pb^{2+}-induced UV spectral changes. [Cesium 4-methylbenzoate] = 5.0 x 10^{-5} mol/L (in water).

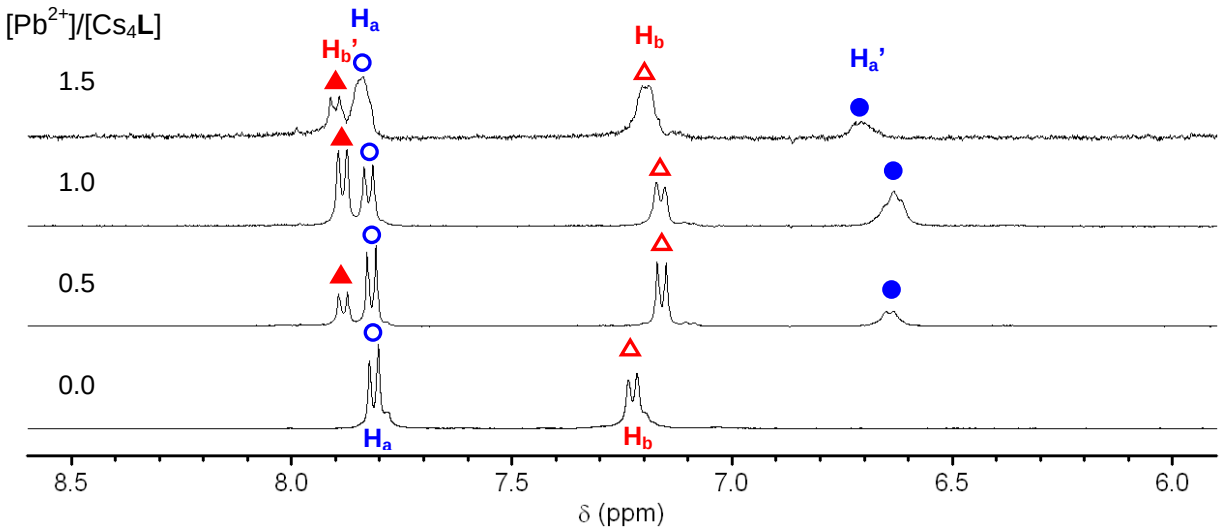

Figure S17. $Pb(NO_3)_2$-induced ^{1}H-NMR spectral changes (D_2O, 298 K).

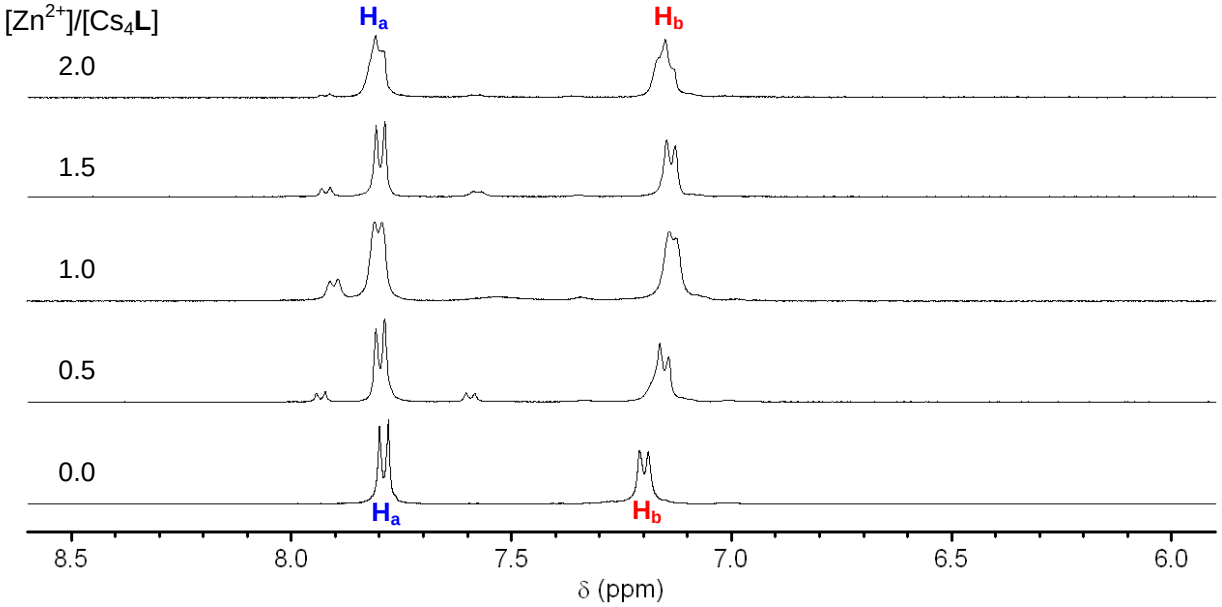

Figure S18. $Zn(NO_3)_2$-induced ^{1}H-NMR spectral changes (D_2O, 298 K).

Table S3 ^{1}H NMR chemical shift changes of the protons at 2'-/6'- positions (δ/ppm).

$LiNO_3$	-0.01
$NaNO_3$	-0.01
KNO_3	-0.01
$Mg(NO_3)_2$	-0.04
$Ca(NO_3)_2$	-0.06
$Sr(NO_3)_2$	-0.01
$Co(NO_3)_2$	-0.00
$Ni(NO_3)_2$	-0.03
$AgNO_3$	**-0.72**
$Zn(NO_3)_2$	-0.06

Negative values denote higher-field shifts.

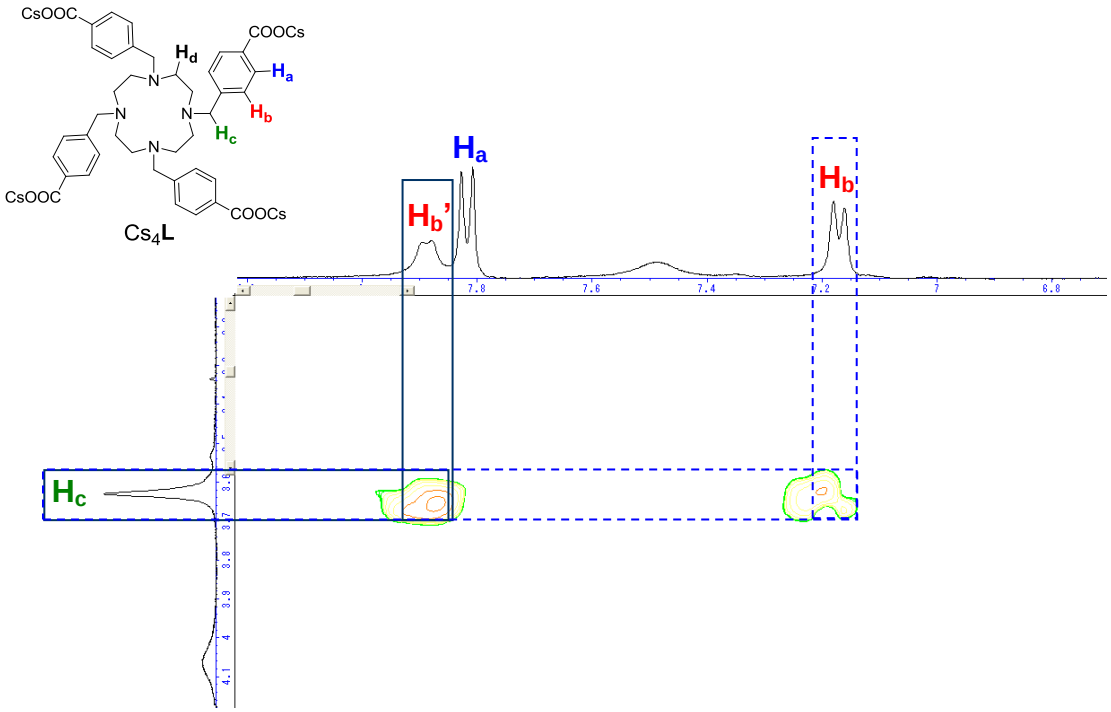

Figure S19. ^{1}H-^{1}H HOHAHA NMR $[Pb^{2+}]/[Cs_4\mathbf{L}]$ = 0.5 in $CDCl_3/CD_3OD$.

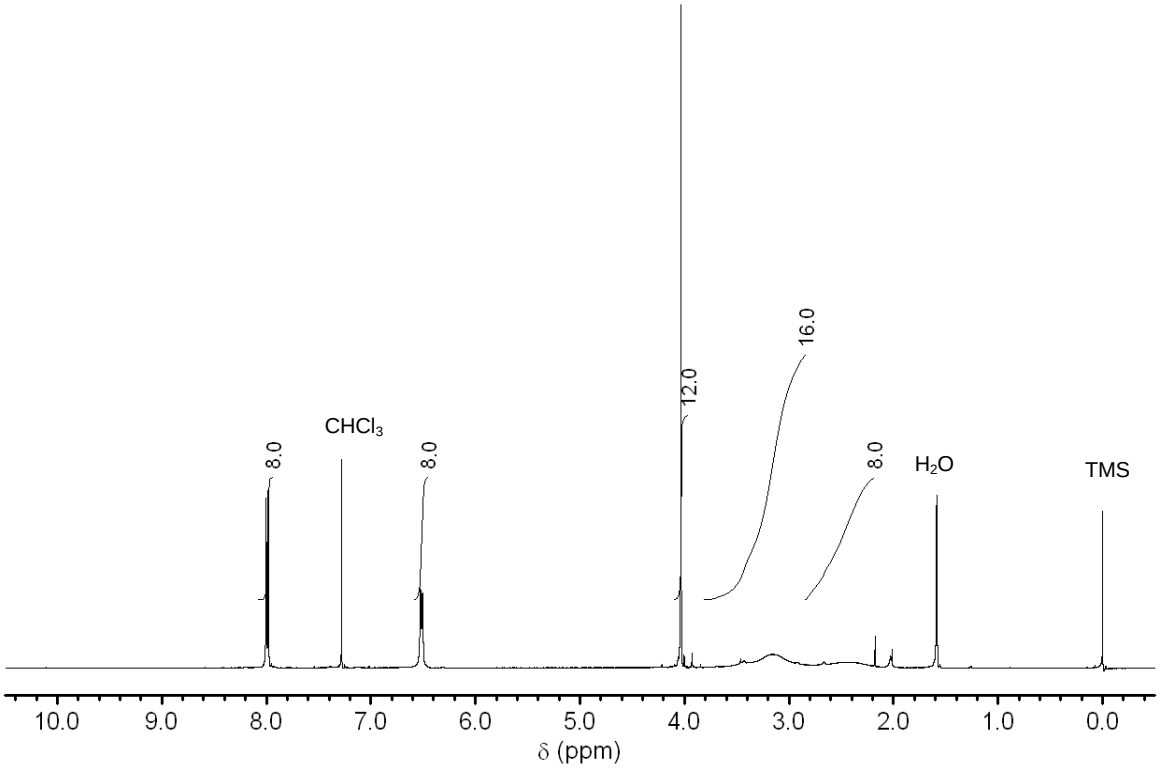

Figure S20. ^{1}H NMR of a 1:1 mixture of tetramethy 4,4',4",4"'-[1,4,7,10-tetraazacyclododecane-1,4,7,10-tetrayltetrakis(m-ethylene)]tetrabenzoate (**3**) and $AgCF_3SO_3$ ($CDCl_3$/CD_3OD, 298 K).

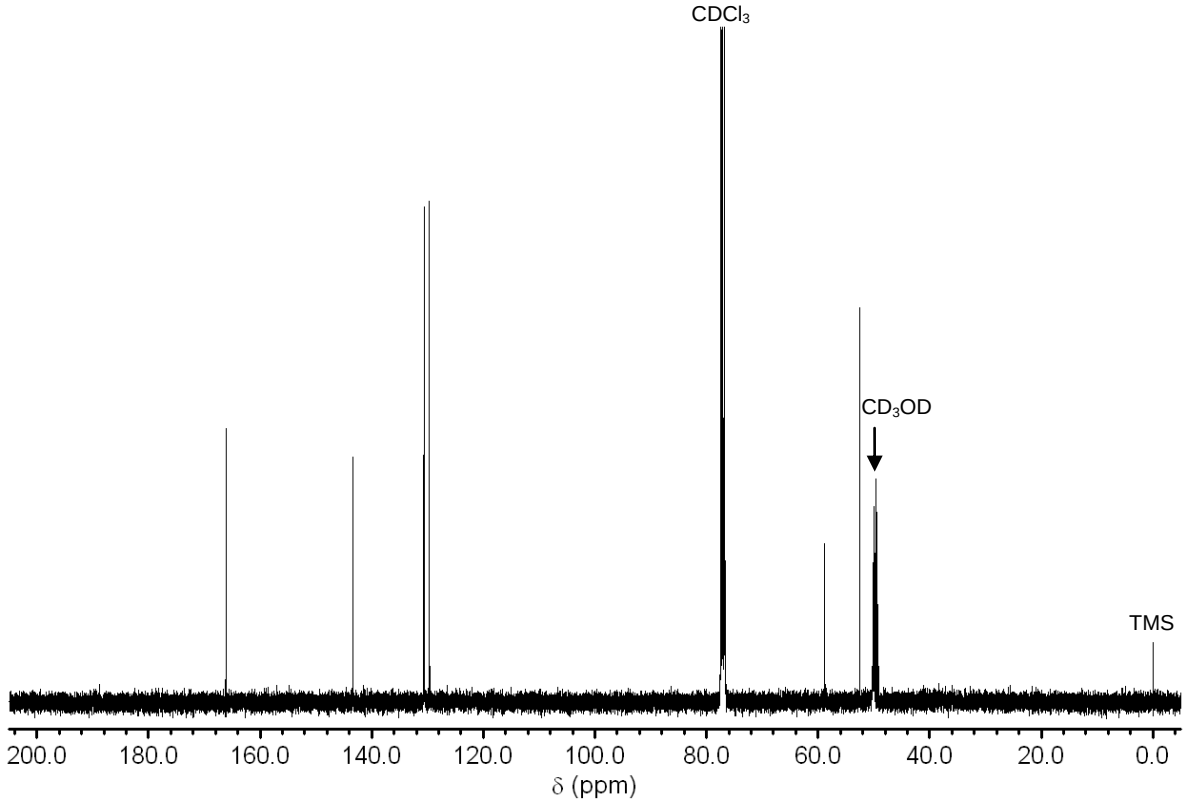

Figure S21. ^{13}C NMR of a 1:1 mixture of tetramethy 4,4',4",4"'-[1,4,7,10-tetraazacyclododecane-1,4,7,10-tetrayltetrakis(m-ethylene)]tetrabenzoate (**3**) and $AgCF_3SO_3$ ($CDCl_3$/CD_3OD, 298 K). The ^{13}C siglnals of the CF_3SO_3 anions was not observed under the conditions.

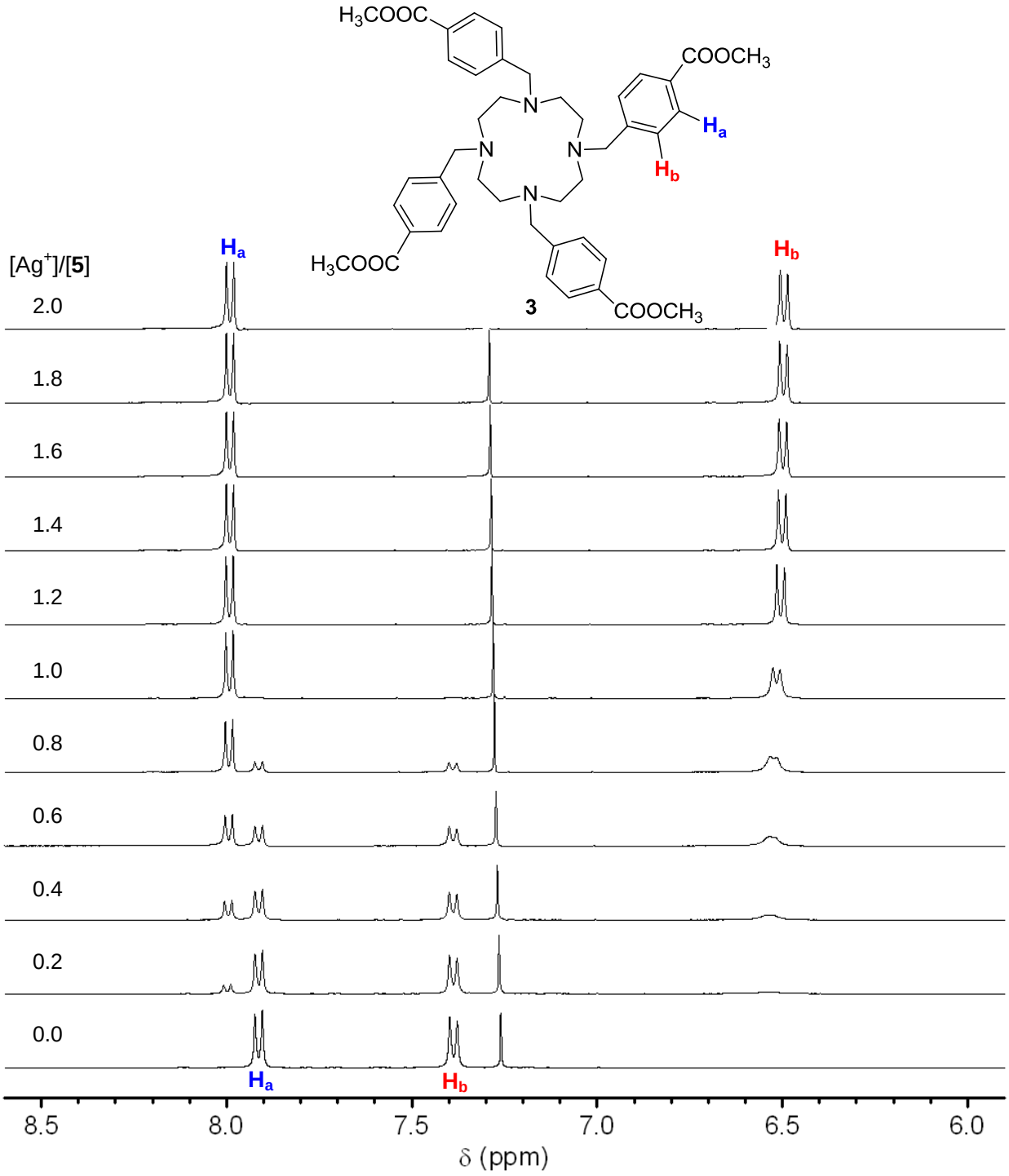

Figure S22. $AgCF_3SO_3$-induced ^{1}H-NMR spectral changes ($CD_3OD/CDCl_3$, 298 K). The H_b (2'-/6'-positions) and H_a (3'-/5'-positions) protons were shifted to higher and lower field by ca. –0.87, and + 0.08 ppm, respectively.

Table S4. Crystal data and structure refinement for **3**/$AgCF_3SO_3$.

Identification code	**3**/$AgCF_3SO_3$.	
Empirical formula	C90 H106 Ag2 F6 N8 O23 S2	
Formula weight	2061.69	
Temperature	120 K	
Wavelength	0.71073 Å	
Crystal system	Tetragonal	
Space group	P4/n	
Unit cell dimensions	a = 13.997(4) Å	α= 90°.
	b = 13.997(4) Å	β= 90°.
	c = 23.804(6) Å	γ = 90°.
Volume	4664(2) $Å^3$	
Z	2	
Density (calculated)	1.468 Mg/m^3	
Absorption coefficient	0.553 mm^{-1}	
F(000)	2132	
Crystal size	0.21 x 0.20 x 0.10 mm^3	
Theta range for data collection	0.86 to 28.33°.	
Index ranges	-18<=h<=18, -18<=k<=18, -31<=l<=18	
Reflections collected	34383	
Independent reflections	5822 [R(int) = 0.0542]	
Completeness to theta = 28.33°	99.6 %	
Absorption correction	Empirical	
Max. and min. transmission	0.9462 and 0.8913	
Refinement method	Full-matrix least-squares on F^2	
Data / restraints / parameters	5822 / 0 / 332	
Goodness-of-fit on F^2	1.130	
Final R indices [I>2sigma(I)]	R1 = 0.0562, wR2 = 0.1381	
R indices (all data)	R1 = 0.0723, wR2 = 0.1502	
Largest diff. peak and hole	1.793 and -0.814 e.$Å^{-3}$	

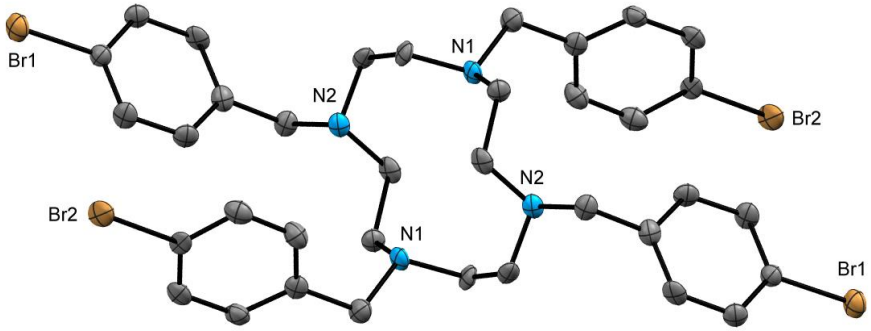

Figure S23. ORTEP diagram of **5**. Hydrogen atoms are omitted.

Table S5. Crystal data and structure refinement for **5**.

Identification code	**5**	
Empirical formula	C36 H40 Br4 N4	
Formula weight	848.36	
Temperature	100 K	
Wavelength	0.71073 Å	
Crystal system	Triclinic	
Space group	P-1	
Unit cell dimensions	a = 7.399(3) Å	α= 95.954(8)°.
	b = 9.641(5) Å	β= 96.675(8)°.
	c = 12.392(6) Å	γ = 96.258(8)°.
Volume	866.7(7) $Å^3$	
Z	1	
Density (calculated)	1.625 Mg/m^3	
Absorption coefficient	4.675 mm-1	
F(000)	424	
Crystal size	0.29 x 0.22 x 0.20 mm^3	
Theta range for data collection	1.67 to 27.48°.	
Index ranges	-9<=h<=8, -12<=k<=11, -14<=l<=16	
Reflections collected	5174	
Independent reflections	3794 [R(int) = 0.0420]	
Completeness to theta = 27.48⌐	95.4 %	
Absorption correction	Empirical	
Max. and min. transmission	0.4579 and 0.3442	
Refinement method	Full-matrix least-squares on F^2	
Data / restraints / parameters	3794 / 12 / 199	
Goodness-of-fit on F2	1.022	
Final R indices [I>2sigma(I)]	R1 = 0.0966, wR2 = 0.2542	
R indices (all data)	R1 = 0.1281, wR2 = 0.2815	
Largest diff. peak and hole	3.941 and -2.395 e. $Å^{-3}$	

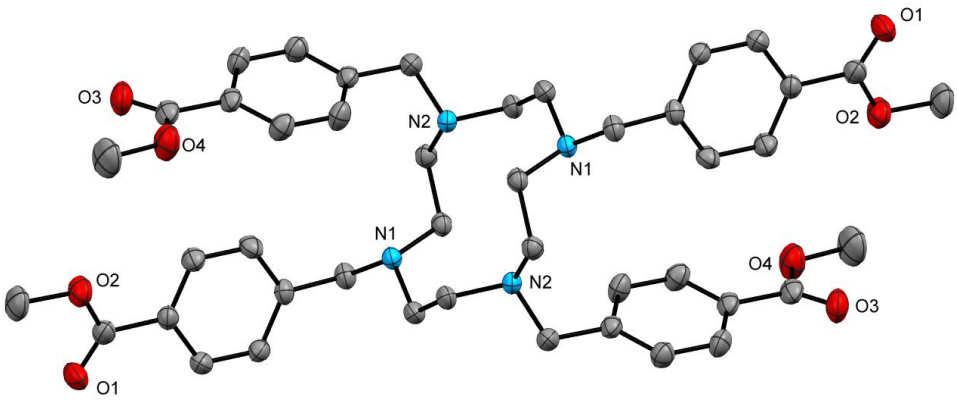

Figure S24. X-ray structure of **3**. Hydrogen atoms are omitted.

Table S6. Crystal data and structure refinement for **3**.

Identification code	**3**	
Empirical formula	C44 H52 N4 O8	
Formula weight	764.90	
Temperature	173 K	
Wavelength	0.71073 Å	
Crystal system	Triclinic	
Space group	P-1	
Unit cell dimensions	a = 10.0192(9) Å	α= 110.849(2)°.
	b = 10.1213(9) Å	β= 103.926(2)°.
	c = 11.6590(11) Å	γ = 103.909(2)°.
Volume	1000.74(16) $Å^3$	
Z	1	
Density (calculated)	1.269 Mg/m^3	
Absorption coefficient	0.088 mm^{-1}	
F(000)	408	
Crystal size	0.48 x 0.36 x 0.21 mm^3	
Theta range for data collection	2.30 to 28.27°.	
Index ranges	-13<=h<=13, -11<=k<=13, -15<=l<=12	
Reflections collected	7524	
Independent reflections	4903 [R(int) = 0.0181]	
Completeness to theta = 28.27⁻	98.7 %	
Absorption correction	Empirical	
Max. and min. transmission	0.9817 and 0.9594	
Refinement method	Full-matrix least-squares on F^2	
Data / restraints / parameters	4903 / 0 / 255	
Goodness-of-fit on F^2	1.022	
Final R indices [I>2sigma(I)]	R1 = 0.0529, wR2 = 0.1359	
R indices (all data)	R1 = 0.0693, wR2 = 0.1477	
Largest diff. peak and hole	0.342 and -0.195 e. $Å^{-3}$	

Figure S25. Calculation of log*K* from UV-vis titration experiments. [Cs_4**L**] = 5.0 x 10^{-5} mol/L (in water)

	A	B	C	D	E	F	G	H
1	Ag+/Ligand	Absorabance/ Experimental	Lt*(A2+1)+1 /K	SQRT(C2^2-4*A2*Lt^2)	ML	Xfree	Absorabance /Calcd	diff^2
2	0	2.02461	5.0065E-05	5.0065E-05	0	1	2.02461	0
3	0.1	1.99333	5.50715E-05	4.50585E-05	5.0065E-06	0.90000004	1.996380262	9.3041E-06
4	0.2	1.95993	6.0078E-05	4.0052E-05	1.0013E-05	0.80000009	1.968150526	6.7577E-06
5	0.3	1.9303	6.50845E-05	3.50455E-05	1.50195E-05	0.70000016	1.939920795	9.256E-05
6	0.4	1.89889	7.0091E-05	3.0039E-05	2.0026E-05	0.60000025	1.91169107	0.00016387
7	0.5	1.86819	7.50975E-05	2.50326E-05	2.50325E-05	0.50000037	1.883461355	0.00023321
8	0.6	1.83815	8.0104E-05	2.00261E-05	3.0039E-05	0.40000056	1.855231658	0.00029178
9	0.7	1.8065	8.51105E-05	1.50196E-05	3.50455E-05	0.30000087	1.827001995	0.00042033
10	0.8	1.7775	9.0117E-05	1.00132E-05	4.00519E-05	0.20000149	1.79877242	0.00045252
11	0.9	1.74559	9.51235E-05	5.00685E-06	4.50583E-05	0.10000335	1.770543195	0.00062266
12	1	1.74019	0.00010013	6.10748E-08	5.00345E-05	0.00060977	1.742484636	5.2654E-06
13	1.1	1.7385	0.000105137	5.00689E-06	5.00648E-05	3.7203E-06	1.74231355	1.4543E-05
14	1.2	1.74064	0.000110143	1.00132E-05	5.00649E-05	1.8602E-06	1.742313025	2.799E-06
15	1.6	1.74361	0.000130169	3.00391E-05	5.0065E-05	6.2007E-07	1.742312675	1.6831E-06
16	2	1.7465	0.000150195	5.00651E-05	5.0065E-05	3.7205E-07	1.742312605	1.7534E-05
17							sum(diff^2)	0.00239564
18	K	53687092200	10.73	0.00239564				
19	d_comp	1.74231						
20	Lt	0.000050065						

	logK	K	sum(diff^2)
24	9.8	6368709220	0.004380198539
25	9.9	7368709220	0.004380105722
26	10.0	9368709220	0.004379985061
27	10.0	10368709220	0.004379844146
28	10.1	11368709220	0.004379911394
29	10.3	21368709220	0.004379770645
30	10.7	51368709220	0.004379711527
31	10.8	61368709220	0.004379708986
32	10.8	66368709220	0.004379708452
33	10.9	71368709220	0.004379708229
34	10.9	73368709220	0.004379708208
35	10.9	73868709220	0.004379708208
36	10.9	74368709220	0.004379708209
37	10.9	76368709220	0.004379708235
38	10.9	81368709220	0.004379708408
39	10.9	86368709220	0.004379708705
40	11.0	91368709220	0.004379709094
41	11.0	1.01369E+11	0.004379710059
42	11.2	1.51369E+11	0.004379715986
43	11.3	2.01369E+11	0.004379721491

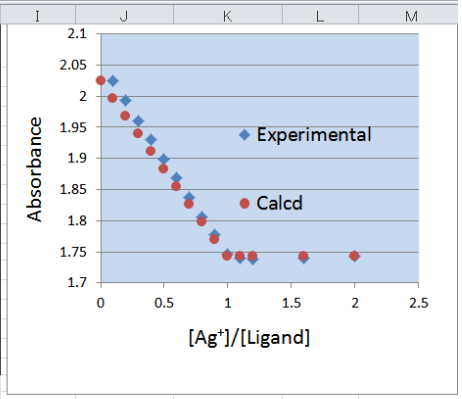

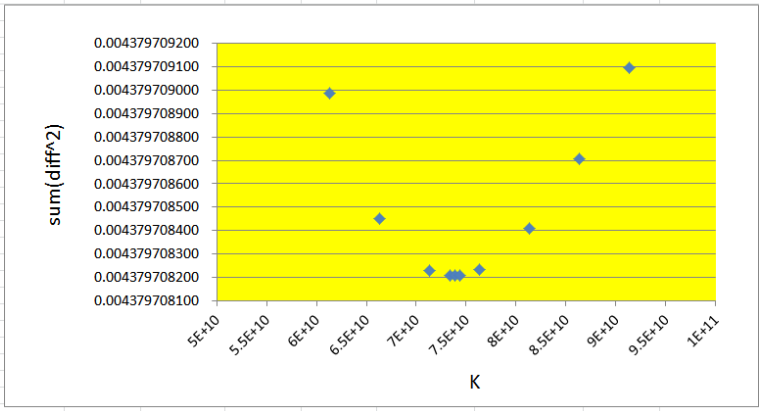

Figures S25 shows Ag^+-ion-induced UV spectral changes of Cs_4**L**. Nonlinear least-squares analyses of the titration profiles clearly indicated the formation of 1:1 complexes, and allowed us to estimate the association constants. The log*K* value between Cs_4**L** and Ag^+ ions in wate was estimated to be ca.10.9.